$$A_1 = (A_1^{(0)} + A_1^{(+2)} e^{2i\omega_0 t} + A_1^{(-2)} e^{-2i\omega_0 t}) e^{i\omega t} + \cdots .$$

We have kept only the dominant terms driven by the resonance $\omega_0 \sim \omega_p$. On the left-hand side of Eq. (2) we keep only the $k^2c^2A_1$ term, with the approximation $kc \gg \omega_p$. The solution for A_1 is then substituted into Eq. (1). The γ factors on the right-hand side of Eq. (1) can be neglected to the order of interest, and expanded to order v_0^2/c^2 on the left-hand side. Thus the electron density fluctuations at $\pm\omega_0$ are coupled by the incident E_0 through relativistic mass corrections and through the $\vec{v}\times\vec{B}$ force. The dispersion relation becomes

$$\omega^2 = (\omega_p^2 - \omega_0^2 + 3k^2KT/m - \tfrac{3}{4}v_0^2\omega_0^2/c^2)^2/4\omega_0^2 - \omega_0^2 v_0^4/256c^4 . \quad (3)$$

The maximum growth rate is[3,4]

$$\omega_I = \tfrac{1}{16}\,(v_0^2/c^2)\;\omega_0 ,$$

when the bracket in Eq. (3) equals zero. As ω_{pe} approaches ω_0, the most unstable wave number satisfies $k^2c^2 = \omega_0^2 v_0^2/4v_t^2 \gg \omega_0^2$. Since the incident light satisfies the approximate equation $k_0^2c^2 = \omega_0^2 - \omega_p^2$, we were justified in ignoring the wavelength dependence of the incident light. [The modified two-stream instability has a maximum growth rate given by $\omega_I^3 = 0.17\;\omega_{pi}^3\,(M/m)^{1/2}$.]

Energy is being deposited in both the transverse electromagnetic wave E_t and in the longitudinal electrostatic wave E_l. The ratio of the two can also be found from Eqs. (1) and (2):

$$E_l/E_t \cong (c/v_0)\,(kc/\omega_0) \gg 1.$$

Most of the energy will be deposited in the longitudinal plasma oscillations. The wave vector $\vec{k}_0$ of the laser light can be paralled to $\vec{k}$ or parallel to $\vec{B}_t$. If $\vec{k}$ is perpendicular to the plasma density gradient, then the effects of the plasma density gradient should be minimized.

---

*Work performed under the auspices of the U. S. Atomic Energy Commission.

[1]K. Nishikawa, J. Phys. Soc. Japan 24, 4 (1968).
[2]V. P. Silin, Zh. Eksperim. i Teor. Fiz. 48, 1679 (1965) [Sov. Phys. JETP 21, 1127 (1965)].
[3]J. Sanmartin, Phys. Fluids 13, 1533 (1970).
[4]N. L. Tsintsadze, Zh. Eksperim. i Teor. Fiz. 59, 1251 (1971) [Sov. Phys. JETP 32, 684 (1971)].

PHYSICAL REVIEW A VOLUME 5, NUMBER 1 JANUARY 1972

Motion of Ions in Helium II

Timothy C. Padmore*
School of Physics, Georgia Institute of Technology, Atlanta, Georgia 30332
(Received 29 June 1971)

The general motion of ions in He II is investigated assuming that nucleation of and escape from vortex rings is a random thermally activated process. The mean drift velocity v_d is calculated as a function of temperature, applied field, and ionic species. It is shown that low-field data up to and just beyond the giant discontinuity can be explained, provided careful attention is paid to the friction forces on small rings, by assuming that v_d is the equilibrium drift velocity. The transition between bare-ion and vortex-ring behavior is discussed in some detail. At higher fields one must take into account vortex-ring dynamics and the possibility of escapes. In general v_d is larger than the equilibrium velocity and, for very large fields, increases with field. Predictions of the theory are compared with experimental drift-velocity data. Also considered are the characteristics of ion currents in nonuniform fields. In particular, predictions are made for the "persistence current" observed when ions propagate first through a region of constant field, then through a region of zero or retarding field.

I. INTRODUCTION

The diversity and novelty of problems associated with the motion of ions in superfluid helium has made this subject a popular area of investigation for both theorists and experimenters. The diversity arises because the ion has separate and quite different interactions with the normal and the superfluid components. The relevant physical processes have been mostly identified, however, and the main features of ion motion can now be understood. It is the purpose of this paper to discuss the interplay of these processes and to present quantitative calculations of the average ion drift velocity and persistence currents.

The main physical effects governing the motion of an ion under the influence of an electric field are the viscous force on a bare ion, the possibility the ion will nucleate and be captured by a quantized vortex ring, the electric and viscous forces on the

ion-ring complex, and the possibility the ion will escape from the ring. Depending on the temperature and the applied field, different combinations of these effects (in some cases all of them) are important in determining the motion of the ion.

In Sec. II we discuss the ion drift velocity in terms of the standard picture in which the bare ion or ion-ring system moves with a constant equilibrium velocity. Special attention is paid to the viscous force on an ion trapped in a "small" ring. In Secs. III and IV we discuss two regions in which the simple equilibrium picture breaks down. The discussion in Sec. III of the transition region between bare-ion equilibrium and ion-ring equilibrium includes an analysis of the effect on the average drift velocity of the dynamic instability first noted by Huang and Olinto.[1] In Sec. IV we discuss ion motion in large electric fields where the peculiarities of vortex-ring dynamics and the possibility of the ion escaping from its ring make equilibrium a rarity. Formulas are derived giving the average drift velocity v_d in these circumstances. Extensions to account for small-ring dynamics and other effects are discussed and applied to an analysis of experimental data. In Sec. IV we also discuss the "persistence current" observed[2] when ions propagate first through a region with a large constant field, and then through a (macroscopic) region of zero or retarding field.

Summaries of definitions used in the text may be found at the end of Secs. III and IV.

II. IONS AND RINGS IN EQUILIBRIUM

In a typical experiment ions of negligible energy enter a region of constant and uniform electric field. The ions move in the field, gaining energy, for a fixed distance d and are then collected. A variety of methods[3] can be used to determine the mean time τ_d it takes the ions to negotiate the distance d, and hence the average drift velocity $v_d \equiv d/\tau_d$.

A. Motion of Bare Ion

In small electric fields the ion behaves as it would in a simple fluid, v_d increasing with field and the mobility steadily decreasing (Fig. 1). The similarity to the behavior one would expect in an ordinary viscous fluid makes plausible the assumption that the motion of the ion is governed by a balance between the electric force eE and a mean viscous drag force $f_{\rm ion}(v)$, where v is the instantaneous velocity. The equation of motion of the ion is

$$M_{\rm ion}\dot{v} = eE - f_{\rm ion}(v) \ . \tag{2.1}$$

According to this picture the ion accelerates from rest and asymptotically approaches the limiting velocity $v_{\rm eq}^{\rm ion}$ given by

$$eE - f_{\rm ion}(v_{\rm eq}^{\rm ion}) = 0 \ . \tag{2.2}$$

One can estimate from Eq. (2.1) that the equilibrium velocity is achieved in a distance somewhat greater than $\frac{1}{2}M_{\rm ion}v_{\rm eq}^{\rm ion\ 2}(eE)^{-1}$, which is the order of $10^{-6}E^{-1}$ cm with E in kV/cm. For the range of fields considered in this paper, from about 1 V/cm up to the order of 10 kV/cm, the latter distance is much smaller than d, which is usually ~ 1 cm. The history of a typical ion is therefore as shown by curves (i) and (ii) of Fig. 2 (a). (The extent of the acceleration regions has been exaggerated in the figures.) It is clear that the average drift velocity $v_d \approx v_{\rm eq}^{\rm ion}$ and v_d is therefore given by

$$eE - f_{\rm ion}(v_d) = 0 \ . \tag{2.3}$$

One sees, incidentally, that the drift-velocity curve, viewed with v_d as the abscissa and eE as the ordinate, is just a plot of $f_{\rm ion}(v)$ vs v.

B. Drag Force on Bare Ion

The drag force can be expanded

$$f_{\rm ion}(v) = e\mu^{-1}v + \cdots \ , \tag{2.4}$$

where the dots indicate terms of higher order in v. Comparison with (2.3) shows that μ is the zero-field mobility defined by $v_d = \mu E$. Strayer *et al.* have calculated[4] large-v corrections to (2.4). The decreased mobility at high velocities is reasonably explained in terms of an enhanced density of rotons in the disturbed region near the ion, giving rise to an increased drag force. Use of the theory with (2.3) yields[4] satisfying agreement with measurements of v_d. These results help confirm the simple equilibrium picture. This point is emphasized because of suggestions[1,5] that the ion generates coherent turbulence of some sort (e.g., vortex rings) and that as a consequence $f_{\rm ion}$ depends on the past history of ion, not just the present velocity. The inspiration for such theories was, of course,

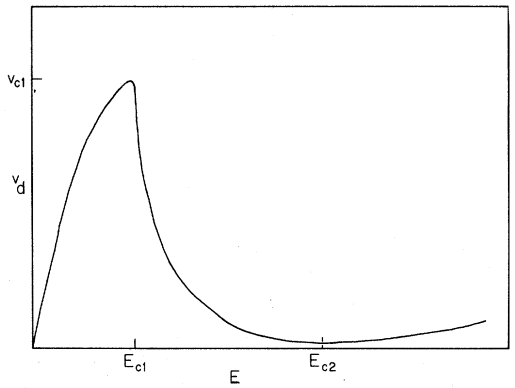

FIG. 1. Typical plot of average ion drift velocity vs applied electric field.

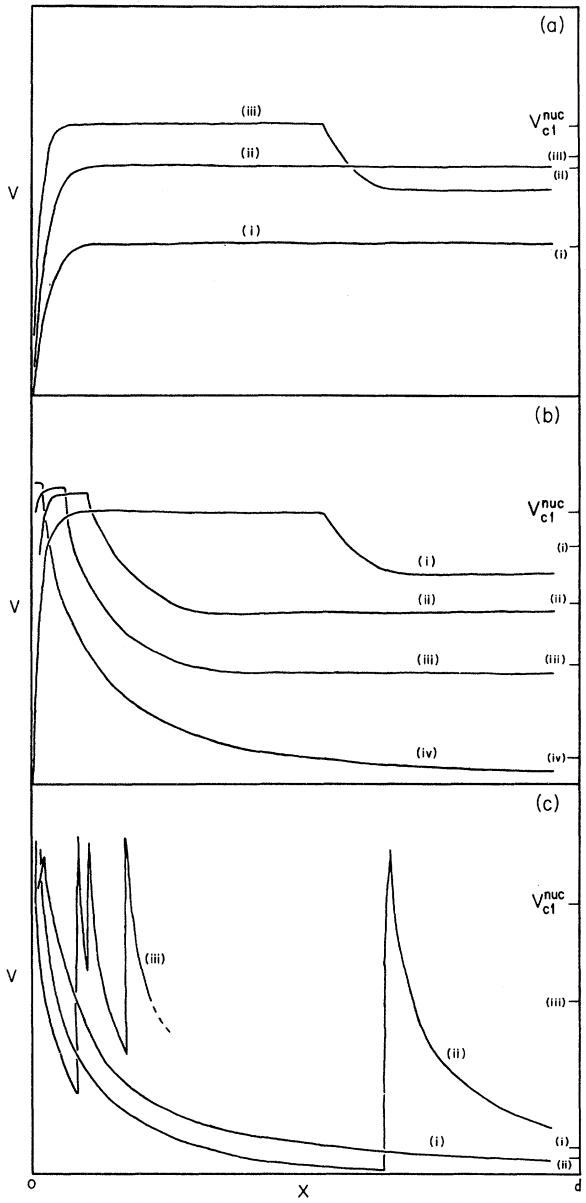

FIG. 2. Characteristic ion histories for a sequence of increasing electric fields: (a) $0 \lesssim E \lesssim E_{c1}$, (b) $E_{c1} \lesssim E \lesssim E_{c2}$, (c) $E_{c2} \lesssim E$. The tick marks labelled (i), (ii), etc., give the time-of-flight average velocity for the corresponding history. Curve (a) (iii) is repeated as (b) (i) and likewise (b) (iv) is repeated as (c) (i). The bare-ion acceleration distance and the deceleration distance for small rings are exaggerated.

the famous "Careri steps" by which the mobility was observed to decrease at regular intervals of the drift velocity. The mobility steps were observed by at least two laboratories[6,7] and frustrated attempts[1,5] at a quantitative theoretical interpretation. However, recent experiments[8] using very direct and reliable techniques for measuring τ_d exhibited no steps at all. It therefore seems likely that the steps are associated with a facet of the experiments other than the central property, i.e., v_d, whose measurement was sought.

C. Beyond the Frist Critical Field

Now consider what happens with higher applied fields. As the electric field is increased, and for temperatures $T \lesssim 1.35\,^{\circ}\mathrm{K}$, one reaches a critical velocity v_{c1} and field E_{c1} beyond which v_d falls precipitately with field.[2,6] (See Fig. 1.) In this region one supposes the ions to be trapped in singly quantized vortex rings.[1,9] On a microscopic scale the motion of the ion is as illustrated by curves (i), (ii), and (iii) in Fig. 2(b).

There is a narrow range of fields such that nucleation of the ring[10] does not occur until the ion has propagated a good fraction of the way across the drift space [curve (i)]. The mean drift velocity of a bare ion at these fields is generally close to v_{c1}. This case is treated in Sec. III below.

At higher fields the history of an ion is as follows. The bare ion accelerates to an equlibrium velocity greater than v_{c1}. Shortly thereafter it nucleates and is captured by a ring, which then grows and decelerates to *its* equilibrium velocity. The equation of motion of the ion-ring complex may be written simply as

$$\dot{p} = F \ , \tag{2.5}$$

where the momentum

$$p = M_{\mathrm{ion}} v + \pi \rho_s \kappa R^2 \tag{2.6}$$

is the sum of the ion momentum and the momentum of the ring. The total force F is $eE - f_{\mathrm{ir}}(v)$, where f_{ir} is the drag force on the ion-ring system. The ring radius R is related to the velocity by the classical formula

$$v = (\kappa/4\pi R)\ln(R/\xi) \ . \tag{2.7}$$

Here and above κ is the circulation, $\kappa = 0.997 \times 10^{-3}$ cm^2/sec, ρ_s is the fluid density and ξ is related to the core radius $a \approx 1$ Å by $\xi = \frac{1}{8} e^{1/4} a$. Once more one expects the ion to approach an equilibrium velocity, given in this case by

$$eE - f_{\mathrm{ir}}(v_{\mathrm{eq}}^{\mathrm{ir}}) = 0 \ . \tag{2.8}$$

The equilibrium velocity[11] is achieved in a distance, subsequent to the nucleation of the ring, of the order

$$\tfrac{1}{2}\rho_s \kappa^2 R_{\mathrm{eq}} [\ln(R_{\mathrm{eq}}/\xi) - \tfrac{3}{2}]/eE \ .$$

The numerator is the energy of the equilibrium ring with R_{eq} related to $v_{\mathrm{eq}}^{\mathrm{ir}}$ as in (2.7). For a wide range of ring sizes this characteristic distance is much less than $d \sim 1$ cm; once more a simple equilibrium picture obtains and the drift velocity $v_d \approx v_{\mathrm{eq}}^{\mathrm{ir}}$. Curves (ii) and (iii) of Fig. 2(b) illustrate the effect of increasing the applied

field—the equilibrium ring size increases and v_d decreases. (Once more the scale of the non-equilibrium parts of the ion history is exaggerated for clarity.)

D. Drag Force on Ion-Ring Complex

Although v_{eq}^{ir} is determined in principle by Eq. (2.8), in practice f_{ir} is not easy to calculate. For large slow rings, however, the situation is comparatively simple with f_{ir} given by[12]

$$f_{ir} \approx f_{ring} = \alpha(T) \ln(R/\xi). \tag{2.9}$$

Here f_{ring} is the drag on the ring alone. All details of the distribution and scattering properties of impurities and excitations of the fluid are contained in the temperature-dependent experimentally well-known coefficient α.

Combining (2.7), (2.8), and (2.9) gives the Careri formula[1,9] in the form

$$v_d = \frac{\kappa}{4\pi\xi} \tilde{E} e^{-\tilde{E}} , \tag{2.10}$$

where $\tilde{E} = eE/\alpha$. For $E > E_{c1}$, the ratio eE/α is always substantially larger than unity so the exponential dominates in (2.10) and v_d falls off very rapidly with field, as indicated in Fig. 1.

If the ring size is comparable to the ion radius R_{ion}, the situation is more complicated. Equation (2.9) is derived by assuming the drag force varies linearly with velocity and with ring size. Because the velocity is no longer much smaller than the Landau critical velocity, even for a ring with *no* trapped ion this assumption will be violated. Furthermore, for small R the relations between v, R, and the momentum of the ring depend on the core structure (we have assumed a solid core). More drastic effects follow from the presence of the ion trapped in the vortex ring. First, the momentum and velocity of the ring will be further modified because of the modified velocity field. And, more importantly, the drag force will be (a) *augumented* by the drag force on the relatively large fast moving ion, and (b) *decreased* according to the amount of the ring perimeter which is occupied by the ion. To complicate things further, one cannot expect that the drag force on the ion will simply be $f_{ion}(v)$ (which is available from the drift-velocity measurements with $E < E_{c1}$). This is because the environment of the trapped ion is entirely different than for the bare ion—the circulating velocity field of the vortex ring is, in the vicinity of the ion, as large as the translational velocity of some 10 or 30 m/sec. Huang and Olinto[1] (referred to hereafter as HO) have estimated that this effect results in a reduction of f_{ion} by a velocity-independent factor $\xi \approx \frac{1}{3}$.[13]

Not all of these complications are of equal importance and we argue that the drag force is adequately represented by

$$f_{ir} = \alpha(T)[1 - (\pi R)^{-1} R_{ion}] \ln(R/\xi) + \xi f_{ion}(v) , \tag{2.11}$$

where f_{ion} is taken from the drift-velocity data for $E < E_{c1}$. The term in square brackets is expected to account for effect (b) above and the term ξf_{ion} is like that suggested by HO to account for (a). Consider the other effects. Because a is still an order of magnitude smaller than R, effects due to core structure, while noticeable, are much smaller than those due to (a) and (b). Donnelly and Roberts[10] (hereafter referred to as DR) have calculated the velocity of a small ring with a trapped ion; we find that the corrections are about the same size as the uncertainty regarding the structure of the core. Also, the velocity of the complex, while substantial, is still only half the Landau velocity (~ 60 m/sec) and we do not expect an important deviation from linearity of the dependence of f_{ring} on v and R.

E. Comparison with Experiment

To check the consistency and completeness of (2.11) that expression was used for a least-squares fit to drift-velocity data[14] for E just greater than E_{c1}, allowing α, R_{ion}, and ξ to vary as free parameters. If we have omitted important physical effects, or included them wrongly, one might expect that the free parameters will assume "unphysical" values. Some results are shown in Table I. The nominal values were determined as follows: for α, from the HO extrapolation of Rayfield and Reif's low-temperature (< 0.7 °K) measurements[12] of the drag force on large rings (in-

TABLE I. Comparison of drag force parameters determined by least-squares fit to drift-velocity data with nominal values determined independently.

		α (eV/cm)		R_{ion} (Å)		ξ	
Ion	Temperature (°K)	Nominal value	Fitted value	Nominal value	Fitted value	Nominal value[a]	Fitted value
Positive	0.89	63	65 ± 1.5	5–8	7.3 ± 1.2	~ 0.2	0.31 ± 0.04
Negative	1.41	2320	2290 ± 65	16	18.6 ± 4.5	~ 0.2	0.16 ± 0.06

[a]See Ref. 13.

cluding a correction for the slight temperature dependence[15] of Δ); for R_{ion} from measurements of low-field mobility[16] and vortex trapping times[17]; for ζ from the estimate of HO.

The fit is not particularly sensitive to the correction factors R_{ion} and ζ. Nevertheless, the best-fit values are sufficiently close to the nominal values to lend credibility to our choice of functional form for f_{ir}.

At the same time Table I lends additional support to the idea that the bare-ion part of the drift-velocity curve is a simple equilibrium curve given by (2.8). HO also obtained a good fit to the v_d curve using (2.11) but with $R_{ion}=0$. But they used, instead of the measured $f_{ion}(v)$, the phenomenological form

$$f_{ion}^{HO} = -eE_0 \ln(1 - v/v_0) \ ,$$

where v_0 is the Landau velocity and $E_0 = v_0\mu^{-1}$. In general f_{ion}^{HO} is less than f_{ion}, so that processes (the creation of large vortex rings) had to be invented which prevent attainment of equilibrium. However, the same feature ($f_{ion}^{HO} < f_{ion}$) means that replacing f_{ion} by f_{ion}^{HO} is roughly equivalent to introducing a nonzero R_{ion} in (2.11)—that is, either procedure reduces f_{ir}, so a reasonable fit to the v_d data for $E > E_{c1}$ is obtained. It is interesting in this connection that Cunsolo and Maraviglia,[18] using (2.11) with f_{ion}^{HO} for f_{ion} and $R_{ion}=0$ to analyze experiments with $0.4\ ^\circ\mathrm{K} < T < 1\ ^\circ\mathrm{K}$, found $\zeta = \frac{1}{3}$ and $\frac{1}{5}$ for positive and negative ions, respectively, in substantial agreement with the results presented in Table I.

III. TRANSITION REGION $v_d \approx v_{c1}$

This is the first region we encounter in which a simple equilibrium picture is inadequate to describe the motion of the ion. Because of complications discussed below we are not yet able to give a quantitative theory of the motion in this region. However, some general points can be made.

A. Nucleation of Vortex Rings

According to DR the nucleation of a ring is a thermally activated process. For an ion travelling with a velocity v, the activation energy $\Delta F(v)$ is taken to be the energy of a ring which, in the presence of the ion, propagates with that same velocity. Since the ring energy, and hence ΔF, go roughly as v^{-1}, the nucleation rate $P_n(v)$ increases rapidly with velocity. A critical velocity v_{c1}^{nuc} is defined by $P_n(v_{c1}^{nuc}) = v_{c1}^{nuc}/d$, that is, by the condition that P_n be the reciprocal of the drift time of a bare ion. In the vicinity of v_{c1}^{nuc}, an adequate approximation for P_n is

$$P_n(v) = \frac{v}{v_{c1}^{nuc}}\ \Omega_n \exp\left(-\frac{\Delta F_0}{k_B T}\ \frac{v_{c1}^{nuc}}{v}\right) \ , \quad (3.1)$$

where $\Delta F_0 = \Delta F(v_{c1}^{nuc})$. The parameter ΔF_0 and the preexponential factor Ω_n can be obtained from DR. The quantity $\Delta F_0/k_BT$ is large (~ 50–100), so that $e^{-P_n(v)d/v}$, which is the probability an ion can propagate the distance d at a velocity v *without* nucleating a ring, changes rapidly from very nearly unity for $v < v_{c1}^{nuc}$ to very nearly zero for $v > v_{c1}^{nuc}$. In the former case $v_d \approx v_{eq}^{ion}$, and in the latter case $v_d \approx v_{eq}^{ir}$.

There is an intermediate region where $v_{eq}^{ion} \approx v_{c1}^{nuc}$ [Figs. 2(a), curve (iii), or 2(b), curve (i)] which is relatively narrow (~ 1 m/sec) but quite observable. In this region we can calculate the the average drift velocity as follows. Assuming that once a ring of the appropriate size is nucleated the capture probability is unity and that the resulting ion-ring complex is stable, the mean drift time is

$$\tau_d = \int_0^{d/v_{eq}^{ion}} P_n(v_{eq}^{ion}) \exp[-P_n(v_{eq}^{ion})\, t] \times [t + (d - v_{eq}^{ion}\, t)/v_{eq}^{ir}]\ dt + \exp[-P_n(v_{eq}^{ion})\, d/v_{eq}^{ion}]\, d/v_{eq}^{ion} \ . \quad (3.2)$$

The second bracketed factor under the integral sign is the transit time should nucleation occur between t and $t+dt$ and the rest of the integrand is the probability of such an event. The second term is the contribution of bare ions that survive the entire distance d. The integral in (3.2) is trivial and the average drift velocity can be written

$$v_d = d/\tau_d = v_{eq}^{ir}\ [1 - (1 - v_{eq}^{ir}/v_{eq}^{ion})\, \delta^{-1}(1 - e^{-\delta})]^{-1} \ , \quad (3.3)$$

where $\delta = P_n(v_{eq}^{ion})\, d/v_{eq}^{ion}$. The predicted v_d changes rapidly, but smoothly, from the "ion" equilibrium curve to the "ir" equilibrium curve.

B. Interpretation of Experiments

Often, however, the situation is not so simple and Eq. (3.3) is not obeyed experimentally. One complication is partly a matter of definitions. Consider an ion pulse of finite width which enters the drift space. If we measure the current at d as a function of time, we will observe the same ion pulse but smeared out in time because some of the ions have nucleated rings and have therefore arrived later than otherwise. The mean drift time given by (3.2) is just the centroid of the smeared-out pulse. However this centroid is not necessarily what is measured experimentally. In Fig. 3 we plot the shape of the pulse at d for several different velocities near v_{c1}^{nuc} and an initial pulse width about one-fifth the difference in transit times of a bare ion and of an ion-ring complex. One can see that in the intermediate region there are two distinct peaks at $t \approx d/v_{eq}^{ion}$ and $t \approx d/v_{eq}^{ir}$; for no field is there a peak "in the middle" where the centroid is located. An experiment, particularly one based on a resonance

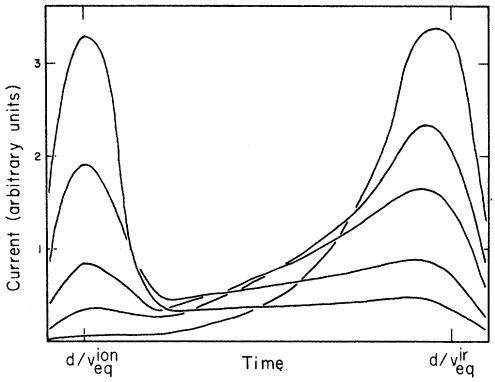

FIG. 3. Collected pulse shapes when $E \sim E_{c1}$, $E > E_{c1}^{HO}$. Left-hand peak is the bare-ion pulse, right-hand peak is the ring pulse.

technique, will tend to measure the location of *one* of the peaks. Hence, experiments generally yield a discontinuity in v_d near E_{c1} (as attention is shifted from one peak to the other) rather than the gentle rounding predicted by (3.3). The reason for this effect is that the beam of bare ions is steadily depleted (by nucleation events) along the drift space. Therefore, more rings are nucleated at the beginning of the drift space than at the end—this accounts for the peak at $t = d/v_{eq}^{ir}$; the remaining fraction, given by the exponential in the second term of (3.2), goes into the bare-ion peak.

C. Dynamic Instability of Ion-Ring Complex

Another complication is that the assumption made just before Eq. (3.2) is not always justified. As pointed out by HO, the frictional force on the ion-ring complex has a minimum for some velocity v_{c1}^{HO}. If an ion-ring complex finds itself in an electric field E smaller than E_{c1}^{HO} (where eE_{c1}^{HO} is the minimum friction force), it will lose energy and break up.[1] Furthermore, even if $E > E_{c1}^{HO}$, the same thing will happen to any ion-ring complex with velocity such that $f_{ir}(v) > E$ and $v > v_{c1}^{HO}$. To see how these ideas are important consider Fig. 4 where we have plotted the drag force f_{ion}, taken from experiment and extrapolated for $v > v_{c1}$, and the drag force f_{ir} on the ion-ring complex calculated from (2.11). The curves are actually taken from data[6] for negative ions at 0.895 °K, but plotted in this fashion, with f normalized against $\alpha(T)$, the curves are to some extent universal because the drag forces on the ring and on the ion change in nearly the same way with temperature. In particular we note that the point where f_{ion} and f_{ir} curves intersect is near $f = eE_{c1}^{HO}$; this is also true for the positive ion.

First, consider the simpler case of an experiment done at a temperature low enough ($\lesssim 1$ °K) that v_{c1}^{nuc} is somewhat (~ 1 or 2 m/sec) greater than v_{c1}^{HO}. We would predict (filled circles in Fig. 4) that the drift velocity will follow the equilibrium curve f_{ion} until the applied field exceeds E_{c1} where $E_{c1} > E_{c1}^{HO}$. At this point there is a fairly sharp discontinuity (depending on the experimental technique and analysis) and thenceforth v_d follows the f_{ir} curve. It is of course possible to observe an ion-ring complex propagating with a velocity appropriate to a field between E_{c1}^{HO} and E_{c1}, but only if it has been nucleated in a field $> E_{c1}$ or captured by a preexisting ring.

Second, consider temperatures high enough so that v_{c1}^{nuc} is smaller than v_{c1}^{HO}. The drift velocity again follows the equilibrium curve until $eE \gtrsim f_{ion}(v_{c1}^{nuc})$. For fields such at $f_{ion}(v_{c1}^{nuc}) \lesssim eE < eE_{c1}^{HO}$, the ion, after it enters the drift space, accelerates and shortly thereafter nucleates and is captured by a ring. The newly formed system is unstable, however, and will lose momentum (and energy) according to Eq. (2.5). The energy $\mathcal{E}_{ir}$ of the

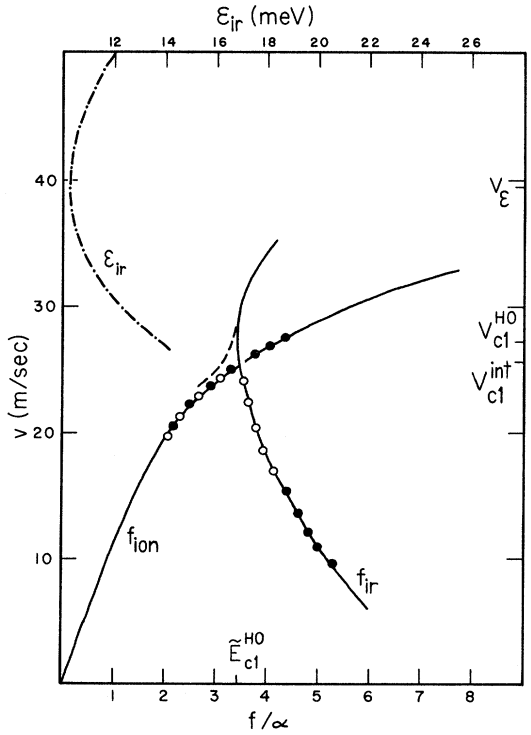

FIG. 4. Drag force on a bare ion and the ion-ring complex (solid curves) and energy of the ion-ring complex (dash-dot curve) as a function of velocity. If the vertical axis is interpreted as drift velocity and the horizontal axis as the reduced field $\tilde{E}$, then the filled circles indicate the behavior of v_d expected at low temperatures, the open circles that at high temperatures. The dashed section shows what happens if v_{c1}^{nuc} is small at low temperatures. The point $(\tilde{E}_{c1}^{HO}, v_{c1}^{HO})$ is the position of the minimum of the function $f_{ir}(v)/\alpha$, and $v_{\mathcal{E}}$ locates the minimum of $\mathcal{E}_{ir}(v)$. The f_{ion} curve intersects the f_{ir} curve at $v = v_{c1}^{int}$.

complex is also plotted in Fig. 4.[19] Like f_{ir}, $\mathcal{E}_{ir}$ has a minimum for some velocity $v_{\mathcal{E}}$. (Note that $v_{\mathcal{E}}$ is relatively large. For the positive ion, because M_{ion} is smaller, $v_{\mathcal{E}}$ is even larger, ~ 50 m/sec.) One therefore expects the ion-ring complex to accelerate to $v_{\mathcal{E}}$ and then, because the complex has no more energy to give up, it must break up. The ion finds itself with a velocity $v > v_{eq}^{ion}$ and therefore decelerates, approaching v_{eq}^{ion} from above. Since the nucleation probability is high, it will shortly nucleate another ring, the complex will accelerate again, break up, and so forth. Typical motion of the ion is illustrated in Fig. 5. The velocity, except during the initial acceleration, is always larger than v_{eq}^{ion}. The average drift velocity v_d is therefore greater than v_{eq}^{ion}. Because the nucleation rate increases with velocity, there will be more high-velocity spikes at higher fields and the difference $v_d - v_{eq}^{ion}$ will tend to increase. Consequently, we expect the drift-velocity curve to look, qualitatively, as indicated by the dashed line in Fig. 4. This feature is, however, not observed at high temperatures. The reason is as follows: Integration of (2.1) and (2.5) shows that, because the frictional and electric forces are so large (~ 10 keV/cm), the high-velocity spikes are very narrow compared to the time between nucleation events. Hence v_d is very close to v_{eq}^{ion} (open circles in Fig. 4). This kind of a feature *has*[20] been observed in dilute He^3-He^4 solutions at low temperatures where the friction forces arise from collisions with He^3 impurities rather than with phonons and rotons. The latter fact alters the nucleation rate[10] and the relationship between the f_{ion} and f_{ir} curves and apparently a situation similar to the one at high temperatures obtains—with the nucleation probability substantial at fields less than E_{c1}^{HO}. Because the friction forces are much smaller, the spikes are much broader, comparable, in fact, to their spacing, and the drift-velocity curve turns upward dramatically just before the sharp fall off where one first forms stable rings.[21]

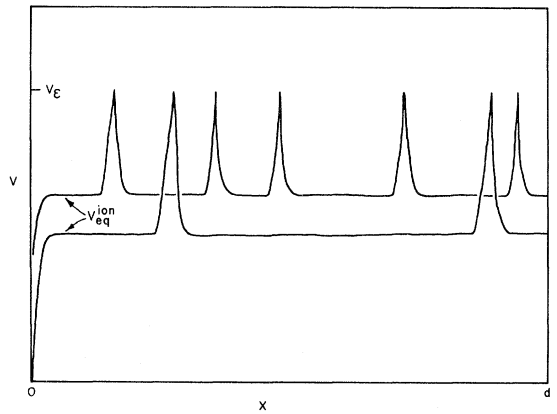

FIG. 5. History of an ion if the nucleation probability is substantial but $E < E_{c1}^{HO}$. The upper curve corresponds to the higher field.

D. Further Complications

The above remarks assume that the critical velocity v_{c1}^{HO} is close to v_{c1}^{int}, the ordinate of the intersection of the f_{ion} and f_{ir} curves (Fig. 4). If v_{c1}^{int} is significantly less than v_{c1}^{HO}, then dynamically stable rings with a velocity v_{eq}^{ir} *larger* than v_{eq}^{ion} can be observed. Provided $P_n(v_{eq}^{ion})$ is large enough, the drift velocity, given by (3.3), will turn *upward*, a feature similar to the one discussed in the last paragraph. It should be possible to distinguish the two cases by the shape of the f_{ir} curve for $v < v_{c1}$. In particular, the effect under discussion may account for some features of Kuchnir's He^3-He^4 experiments at $T \sim 20$ mK.[20] More recent data,[22] however, tend to support the interpretation in Sec. III C.

The consequences of $v_{c1}^{int} > v_{c1}^{HO}$ are less dramatic. Suppose $eE_{c1}^{HO} < eE < f_{ir}(v_{c1}^{int})$, that $P_n(v_{eq}^{ion})$ is substantial, and recall the assumption that when the ring is nucleated it has the same velocity as the ion just before nucleation. Some rings, those nucleated with a velocity v such that $v > v_{c1}^{HO}$ and $f_{ir}(v) > eE$, are dynamically unstable; the balance, a fraction which increases as E increases, will grow to be stable rings with $v = v_{eq}^{ir}$, the smaller root of (2.8). The resulting drift-velocity curve is very similar to the first case discussed in Sec. III C, although the physical description is more complex. Measurements of the upper "unstable" branch of the f_{ir} curve are feasible[23] and would be very helpful in clarifying the physical picture.

Still another complication one finds at high temperatures and fields is the probability of thermally activated escape of the ion from its ring. The consequences of this phenomenon are explored in detail in Sec. IV. The general effect of escapes is clear—since the ion spends more time as a bare ion or in a fast ring, the drift velocity is larger than if there were no escapes.

E. Two Assumptions

Before concluding this section let us briefly examine two tacit assumptions: First, that the interactions of the ion and ion complex with impurities and excitations of the fluid are adequately described in terms of average drag forces f_{ion} or f_{ir}; second, that we can neglect the thermal distribution of energies of different ions.

The assumption that the motion is well described in terms of an average drag force will be valid as long as the ion mean free path λ is small compared to other characteristic distances in the problem, such as the distance in which a ring is nucleated

or the distance it takes for an ion to accelerate to a velocity near v_{eq}^{ion}. The mean free path is given by $\lambda^{-1} = \lambda_r^{-1} + \lambda_\varphi^{-1} + \lambda_3^{-1}$, where λ_r, λ_φ, and λ_3 are the roton, phonon, and He^3 mean free paths, respectively. One estimates $\lambda_{r,\varphi,3} \sim (n_{r,\varphi,3}\sigma_{r,\varphi,3})^{-1}$, where $n_{r,\varphi,3}$ is the roton (phonon) (He^3) number density and $\sigma_{r,\varphi,3}$ the appropriate cross section for scattering from the ion. For $T \gtrsim 0.3\,^\circ$K one can neglect λ_3. Also $\sigma_r \approx \pi R_{ion}^2$ and, because the important phonon wave numbers have $k \gtrsim R_{ion}^{-1}$, $\sigma_\varphi \sim \sigma_r$. In this way we estimate that λ ranges from $\sim 10^{-5}$ cm for $T \sim 0.5\,^\circ$K to $\sim 10^{-6}$ cm for $1.0\,^\circ$K to $\sim 10^{-7}$ cm for $1.5\,^\circ$K. Equation (1.1) has been integrated for a number of fields and temperatures and we find for fields $\sim E_{c1}$ that λ is indeed about an order of magnitude smaller than the characteristic acceleration distance. Ordinarily the bare-ion acceleration distance is the shortest distance in the problem and parameters of interest (such as v_d) are insensitive to it. It is only in experiments at the very lowest temperatures (such as Ref. 20 discussed above) that the mean distance between nucleation events is as small as the acceleration distance. Characteristic distances in situations involving rings are large because of the relatively large energy of a vortex ring. It is only when $E \gg E_{c1}$ that the acceleration distances (and possibly the distance required for a nucleation event) become the order of λ but, as we explain in Sec. IV, the motion of the ion is then dominated by ring dynamics and the ion escape rate.

Regarding the second assumption, we note that the thermal velocity of the bare ions (given by $\frac{1}{2}M_{ion}v_\theta^2 = k_B T$), is the order of 10 m/sec, so we might expect a significant effect on our analysis if the thermal distribution of velocities were properly included. The problem of calculating the velocity distribution, in the presence of a particle sink (nucleation events), of an ion cloud moving with respect to the excitation gas at a velocity comparable to both v_θ and the Landau velocity is theoretically formidable. The resolution of the problem is closely related to the considerations of the previous paragraph. Due to collisions the velocity of an individual ion will fluctuate (by an amount $\sim v_\theta$) around the average velocity of all the ions. If many such fluctuations occur during the interval it takes anything macroscopically interesting (acceleration to v_{eq}^{ion}, nucleation of a ring) to happen, then it is probably a fair first approximation to describe the macroscopically interesting event as if the ion had at all times its average velocity. The comparison of the fluctuation time with the characteristic times of the problem is of course the same one as was concluded in our favor in the previous paragraph.

Note that the mean free path also determines the diffusion of the bare-ion pulse which spreads over a distance $\sim (\tau_d \lambda v_\theta)^{1/2} \sim 10^{-3}$ cm $\ll d$. Corrections due to diffusion of the pulse can therefore be neglected in an ordinary experiment.

F. Summary of Definitions

We have defined a substantial number of special velocities and fields. As an aid in rereading Secs. II and III these definitions are summarized here:

average drift velocity, v_d;
maximum value of v_d just before giant discontinuity, v_{c1};
value of applied field when $v_d = v_{c1}$, E_{c1};
equilibrium bare-ion drift velocity, v_{eq}^{ion};
equilibrium ion-ring drift velocity, v_{eq}^{ir};
Landau critical velocity, v_0;
value of the bare-ion drift velocity for which probability a ring is *not* nucleated is e^{-1}, v_{c1}^{nuc};
value of v for which $f_{ir}(v)$ has a minimum, v_{c1}^{HO};
minimum value of $f_{ir}(v)/e$, E_{c1}^{HO};
velocity where f_{ion} and f_{ir} intersect, v_{c1}^{int};
thermal velocity, v_θ.

IV. HIGH-FIELD BEHAVIOR

We now proceed to consideration of the high field ($E \gg E_{c1}$) behavior. What is observed experimentally is qualitatively as follows. As the electric field is increased v_d falls off, at first as $e^{-eE/\alpha}$, then (at low temperatures) as E^{-1}. For some field E_{c2}, the drift velocity reaches a minimum and subsequently increases approaching a value near v_{c1} for $E \to \infty$ (Fig. 1).

These effects are consequences of vortex-ring dynamics and of the probability that the ion will escape at least once from its ring.

A. Ion-Ring Dynamics

The dynamical behavior is determined by Eq. (2.5). For large rings we can solve this equation completely. If the ring radius R is always large, then we can neglect the contribution of the ion to the momentum and we can take $f_{ir} \approx f_{ring} = \alpha \ln(R/\xi)$ and we obtain

$$2\pi\rho_s\kappa R\,\frac{dR}{dt} = eE - \alpha \ln\left(\frac{R}{\xi}\right) = F\,. \tag{4.1}$$

With the definitions $\tilde{E} = eE/\alpha$, $\tilde{F} = F/\alpha$ one easily finds the time it takes a ring which has just been nucleated to grow to radius R:

$$t(R) = 2\pi\rho_s\kappa\xi^2\alpha^{-1}e^{2\tilde{E}}[\,E_1(2\tilde{F}) - E_1(2\tilde{E})\,]\,. \tag{4.2a}$$

Here E_1 is the exponential integral[25] and the initial condition is $R = \xi$ at $t = 0$. Using the relation $dx = v\,dt$ with the velocity given by (2.7), one obtains in a similar fashion

$$x(R) = \tfrac{1}{2}\kappa^2\rho_s\alpha^{-1}\{\,\xi\tilde{E}\,e^{\tilde{E}}[E_1(\tilde{F}) - E_1(\tilde{E})] - R + \xi\}\,. \tag{4.2b}$$

The functions $x(t)$ and $t(x)$ used below are given parametrically by (4.2a) and (4.2b). The assumption that the ring radius always be large is apparently violated for $t \approx 0$. If the final radius is large, however, the time spent as a "small" ring is a small fraction of $t(R)$ and this error may be neglected. In practice we integrate (2.5) numerically for $R < 100$ Å and use (4.1) when $R > 100$ Å.

In the limit as $\tilde{E} \to \infty$, when dissipative forces can be neglected, Eqs. (4.2) become

$$t(R) = \pi \rho_s \kappa (eE)^{-1} R^2 , \tag{4.3a}$$

$$x(R) = \tfrac{1}{2} \rho_s k^2 (eE)^{-1} R \ln(R/\xi) . \tag{4.3b}$$

[Equations (4.3) are most simply obtained by setting $\alpha = 0$ in (4.1) and integrating directly.] Since $\tilde{E}$ is already ~5 for $E = E_{c1}$, the limiting behavior can be seen for relatively modest fields, say, $E \gtrsim 2E_{c1}$.

The equilibrium radius, given by $eE = \alpha \ln(R/\xi)$, increases exponentially with field. The energy of the equilibrium ring therefore also goes up exponentially with E. The available energy, however, is less than eEd, so clearly if E is very large, the maximum radius R_{max} will be very much smaller than the equilibrium radius. Indeed, if $d \sim 1$ cm, this situation generally occurs for fields a few times E_{c1}; the effect is most pronounced at low temperatures since the available energy for a given $\tilde{E}$ is smaller. This situation, where the equilibrium velocity is never attained, is illustrated by the ion history sketched in Fig. 2(b), curve (iv).

The maximum radius is given by $x(R_{max}) = d$ and from (4.3b) we see that when $\tilde{E}$ and R_{max} are large R_{max} is nearly proportional to E. Consequently, by (4.3a), the drift time

$$\tau_d = t(R_{max}) \propto E , \tag{4.4}$$

so that the average velocity $v_d = d/\tau_d$ goes as E^{-1}.

Implicit in our description of ring dynamics is the assumption that the ring reacts as though uniformly charged. The time required for the ion to diffuse around the ring is $\sim R^2 (v_\theta \lambda)^{-1}$. The dynamical description is certainly justified if this time is substantially less than the time required for the ring to propagate a distance $\sim R$. Hence we obtain the condition $(\lambda v_\theta)^{-1} \kappa \ln(R/\xi) \ll 1$, which is definitely satisfied for low temperatures. (Note the weak R dependence.) The criterion may not be satisfied for $T \gtrsim 1\,^\circ$K; one still has recourse, however, to the following argument: Suppose a force directed along the axis of the ring is applied locally on its perimeter via a trapped ion. This will generate an opposite Magnus force and the element of core will move radially outward, in this way decreasing the local curvature. Hence it will slow down relative to the rest of the ring. The ring is bent so that the electric field now has a component along the core of the ring. The ion is at a point of unstable equilibrium and will be driven along the core toward the opposite side of the ring. The effect, therefore, serves to co-ordinate the motion of different parts of the ring so we can apply the simple dynamical description. The time involved is $\sim R/v_{eq}^{ion}$ and the above criterion is replaced by the condition $(v_{eq}^{ion} R)^{-1} \kappa \ln(R/\xi) \ll 1$, which is readily satisfied.

B. Thermally Activated Escapes

Even though the ion-ring complex may be completely stable with respect to the averaged forces, there is a finite probability that the ion will escape from its ring due to thermal fluctuations.

In the presence of the electric field E the ion is bound to a ring with an energy $W(|E|)$ which can be estimated from classical hydrodynamics.[17] If the escape is thermally activated, one expects the escape rate P_e to have to form

$$P_e = \Omega_e \exp[-W(|E|)/(k_B T)] . \tag{4.5}$$

There have been few experiments measuring P_e directly. In this work Cade's analysis of his positive-ion escape data[26] was used to obtain the approximate form

$$W/k_B \approx (\rho_s/\rho)(15.9 - 1.44|E| + 0.04E^2)$$

and $\Omega_e \approx 1.5 \times 10^{10}$ sec^{-1}. Here ρ_s/ρ is the superfluid fraction and W/k_B has units of °K and E units of kV/cm. The fit is for data taken with $E \sim 10$ kV/cm and $T \sim 0.5\,^\circ$K.

Only zero-field data are available for negative ions and it is not possible to extract a formula similar to (4.5). It is possible to obtain some estimates as follows. From the hydrodynamic analysis[17] one can see that the zero-field binding energy will scale roughly as $R_{ion}^{-} \ln(R_{ion}/a)$, and the coefficients of the higher-order terms roughly as R_{ion}. Using $R_{ion}/R_{ion}^{+} \approx \frac{16}{6}$ and fitting Ω_e to zero-field data,[27] one obtains, for negative ions, $\Omega_e \approx 2.6 \times 10^{11}$ sec^{-1} and

$$W/k_B \approx (\rho_s/\rho)(61.5 - 3.84|E| + 0.11E^2) .$$

This very crude estimate may be expected to give results accurate only to within a couple of orders of magnitude and, as is also the case for the positive-ion formula, only for E not larger than ~15 kV/cm. However, because the escape rate changes by very many orders of magnitude over the accessible ranges of field and temperature, such an estimate can still provide useful information. (For example, see Sec. IV J below.)

In general, escapes are important when $P_e \gtrsim \tau_d^{-1}$. For positive ions, given fields of a few kV/cm, the effect of escapes will be seen down to temperatures ~0.5 °K. At temperatures above ~1 °K the effects of escapes are inevitable at all fields for which dynamically stable rings can be observed.

The negative ion is much more tightly bound. The classical theory tells us that the negative-ion escape probability is significant only for fields $\gtrsim 20$ kV/cm or temperatures $\gtrsim 1.5\,^{\circ}$K where the temperature dependence of ρ_s causes P_e to increase rapidly. At some very large field E_{c3} (~ 40 kV/cm for negative ions and about half that for positive ions), the potential well binding the ion to the ring is completely overwhelmed by the electric field and $P_e \to \Omega_e$. For fields approaching E_{c3} the escape rate will be large even for very low temperatures.

Escapes provide the explanation for the minimum in the drift-velocity curve at E_{c2} and the subsequent rise in v_d. After it escapes, the bare ion accelerates once more to a velocity near v_{c1} and is captured by a new ring which then commences growing toward its equilibrium radius. This sequence of events can be repeated many times. The average velocity of an ion propagating in this fashion is obviously larger than if it had remained trapped in the original ring. If escapes become sufficiently numerous—a situation which inevitably occurs if one goes to high enough fields—then the average drift velocity will increase with field, eventually approaching a velocity near v_{c1} as rings are continuously nucleated and shed.

Representative ion histories are illustrated in Fig. 2(c). Curve (i) is supposed to be for a field small enough that P_e is insignificant. In curve (ii) the escape rate $P_e \sim \tau_d^{-1}$ and we see, typically, a single escape. Because of the escape, the average drift velocity is substantially larger than if there had been no escape. Nevertheless, the average velocity for history (ii) is smaller than for history (i). [Note that the time-of-flight average velocity, which can be written as $(d^{-1}\int_0^d v^{-1}\,dx)^{-1}$, is determined by the trajectory average of v^{-1} not v.] In curve (iii) the applied field has increased so there are very many escapes and the average velocity is larger than for either (i) or (ii).

To conclude this section, let us examine the balance of forces on the ion and the ring. The ion is acted on by the drag force, the electric field, and a trapping force F_r exerted by the ring. The trapping force is important because it is $-F_r$ which must be substituted for eE in (4.5) to determine the escape rate. One has

$$eE - \zeta f_{\rm ion} + F_r = M_{\rm ion}\dot{v}$$

or

$$-F_r = eE - M_{\rm ion}\dot{v} - \zeta f_{\rm ion} \,. \tag{4.6}$$

Now $\dot{v}$ goes as $R^{-3}\ln(R/\xi)$ so that for large rings the second term on the right-hand side of (4.6) can be neglected. Similarly for large slow rings $f_{\rm ion}$ is very small as well and $\zeta f_{\rm ion}$ can also be neglected, so that the magnitude of F_r is nearly equal to eE. In fact, it is only for the very smallest rings that the corrections are of any importance. This fact constitutes an important simplification for it means that in most cases the escape rate P_e can be taken to be constant throughout the experiment.

C. Calculation of Drift Velocity

We are now in a position to make quantitative calculations. The problem can be looked at in the following fashion: Because of the presence of two stochastic processes (nucleation of rings and escapes), there are many different possible ion histories, characterized by the number and locations of escape and nucleation events. With each history h is associated a certain total probability P_h. The average value $\langle Q\rangle$ of any quantity can therefore be calculated by the formula

$$\langle Q\rangle = \textstyle\sum_h P_h Q_h \,, \tag{4.7}$$

where Q_h is the value of that quantity for the history h.

For the time being we will assume

$$P_n(v_{\rm eq}^{\rm ion}) \gg P_e \,, \tag{4.8a}$$

$$P_n(v_{\rm eq}^{\rm ion}) \gg \tau_d^{-1} \,. \tag{4.8b}$$

These assumptions together imply that the ion spends most of its time trapped in a vortex ring. Equation (4.8b) is always satisfied if the applied field exceeds E_{c1} by more than a few per cent. Under the same condition (4.8a) is violated only for very high fields or high temperatures. It is also fair to assume that the rings are large enough so that the dynamics can be described by Eqs. (4.2) and so that P_e is constant; this assumption is valid provided only that v_d is not close to v_{c1}, which again means E should not be near E_{c1}.

Because of (4.8), a typical history is completely characterized by the number and position of the escape events. Since P_e is independent of time the probability an escape occurs between t and $t+dt$ is $P_e\exp(-P_e t)dt$, where t is measured from the last nucleation event. The probability $P^{(N)}(t_1, t_2, \ldots, t_N)\,dt_1 dt_2 \cdots dt_N$ of N escapes occurring at successive intervals $t_1, t_2, \ldots, t_N$ is therefore given by

$$P^{(0)} = \exp[-P_e t(d)] \,,$$

$$P^{(N)}(t_1, t_2, \ldots, t_N) = \begin{cases} P_e^N \exp[-P_e(t_1+t_2+\cdots+t_N)]\,\exp[-P_e t(d - x(t_1) - x(t_2) - \cdots - x(t_N))] \,, \\ \qquad\qquad \text{provided } x(t_1)+x(t_2)+\cdots+x(t_N) < d \\ 0, \text{ otherwise} \,. \end{cases} \tag{4.9}$$

The first N factors $P_e \exp(-P_e t_i)$ give the probability escapes occur at the intervals $t_1, t_2, \ldots, t_n$ and the final factor is the probability that the last ring survives to the end of the drift space *without* an escape.

The history dependent quantity is the time of flight $\Delta t^{(N)}$:

$$\Delta t^{(0)} = t(d) ,$$

$$\Delta t^{(N)}(t_1, t_2, \ldots, t_N) = t_1 + t_2 + \cdots + t_N + t(d - x(t_1) - x(t_2) - \cdots - x(t_N)) ,$$

and the mean drift time τ_d is, according to (4.7),

$$\tau_d = P^{(0)} \Delta t^{(0)} + \sum_{N=1}^{\infty} \int_0^{t(d)} dt_1 \int_0^{t(d-x(t_1))} dt_2 \cdots \int_0^{t(d-x(t_1)-\cdots-x(t_{N-1}))} dt_N \times P^{(N)}(t_1, t_2, \ldots, t_N) \Delta t^{(N)}(t_1, t_2, \ldots, t_N) , \quad (4.10)$$

and of course the average drift velocity $v_d = d/\tau_d$.

One interesting feature of (4.10) is that if $P_e t(d)$ is the order of unity, so that most ions suffer no more than one or two escapes, and if E is large enough so an appreciable fraction of the drift space is required for a ring to approach its equilibrium velocity, then τ_d exhibits a significant d dependence. The velocities are generally lower if more distance is available for deceleration; hence, the mean drift velocity is smaller for the larger distance. If there are many escapes on the average, the ions "forget" their early history and the d dependence fades away.

As with Eq. (3.3), some caution is necessary in the application of (4.10). The structure of the latter equation makes it clear that the collected ion pulse will be a superposition of a "zero-escape peak," a "one-escape peak," and so on. Assuming a sharp input pulse, the zero-escape peak is a δ function with $\Delta t = t(d)$; the N-escape peak has finite width and is centered near a (shorter) drift time $\Delta t = (N+1)t(d/(N+1))$. If P_e is such that many escapes are likely, these merge into a single peak centered near $\Delta t = (\bar{N}+1)t(d/(\bar{N}+1))$, where $\bar{N}$ is the average number of escapes. If, however, P_e is such that no more than one or two escapes are likely, then an experiment may resolve the separate contributions from $N=0$, $N=1$, etc.

D. Limit $P_e t(d) \gg 1$

Equation (4.10), while perfectly general (granted our assumptions), is interesting only for $P_e t(d)$, the order of unity. If $P_e t(d) \ll 1$, the theoretical calculation is easy—the first two terms in (4.10) suffice—but the experiment is hard because v_d is increased only a little from the no-escape value. On the other hand, if $P_e t(d) \gg 1$, then the experimental effect is dramatic but numerical evaluation of the multidimensional integrals occurring in the higher-order terms becomes impractical. By taking advantage of the symmetry of $P^{(N)}$ and $\Delta t^{(N)}$, one can reduce the regions of integration somewhat, so that (4.10) becomes

$$\tau_d = P^{(0)} \Delta t^{(0)} + \sum_{N=1}^{\infty} N! \int_0^{t(dN^{-1})} dt_1 \int_{t_1}^{t([d-x(t_1)][N-1]^{-1})} dt_2 \cdots \int_{t_{N-1}}^{t(d-x(t_1)-\cdots-x(t_{N-1}))} dt_N P^{(N)} \Delta t^{(N)} , \quad (4.11)$$

but this is a modest improvement. One can, however, obtain the large P_e behavior directly. If there are many escapes, the average distance a ring survives is given approximately by

$$\langle x \rangle = \int_0^{\infty} dt\, P_e \exp(-P_e t) x(t) . \quad (4.12)$$

The approximation is a consequence of our neglect of a residual d dependence—the fraction of rings surviving for very long times $\sim \tau_d$ is not simply given by $P_e \exp(-P_e t)$. The total fraction of such long-lived rings is very small, however, and the error is negligible. In the same way we find the mean duration

$$\langle t \rangle = \int_0^{\infty} dt\, P_e \exp(-P_e t) = P_e^{-1} .$$

The mean number of escapes is given by $d/\langle x \rangle = \bar{N} = \tau_d/\langle t \rangle$. Solving for the average drift velocity, one finds the simple result

$$v_d = d/\tau_d = \langle x \rangle / \langle t \rangle = P_e \langle x \rangle . \quad (4.13)$$

E. Extensions of Results

The above results can be easily extended to include corrections to compensate the imperfect treatment of small rings and also to allow for the possibility that P_e can be comparable to P_m [violating condition (4.8a)]. If the latter possibility obtains then the time spent as a bare ion is significant. The bare-ion equation of motion (2.1) can be integrated (numerically) to give $T(v)$, the time it takes the ion to achieve the velocity v, and $X(v)$ the distance it travels in that time. The probability that a ring is

nucleated between T and $T+dT$ is[28]

$$P_n(v)\exp[-\int_0^T P_n(v')dT']dT.$$

[In this last expression, and below, v and v' denote $v(T)$ and $v(T')$, respectively.] In essentially all cases[29] P_n and P_e are both large and we can apply the ideas of Sec. IV D. Now we have to consider the bare-ion and ring stages together. The mean distance between escapes is

$$\int\int_0^\infty dt\,dT\,P_e\exp(-P_e t)P_n(v)\exp[-\int_0^T P_n(v')dT'] \times[x(t)+X(T)]=\langle x\rangle+\langle X\rangle\,, \quad (4.14)$$

where

$$\langle X\rangle=\int_0^\infty P_n(v)\exp[-\int_0^T P_n(v')dT']X(T)dT\,.$$

Similarly the mean time interval between escapes is $\langle t\rangle+\langle T\rangle$ with

$$\langle T\rangle=\int_0^\infty P_n(v)\exp[-\int_0^T P_n(v')dT']T\,dt \quad (4.15)$$

and, using the same argument as before, one finds

$$v_d=(\langle x\rangle+\langle X\rangle)/(P_e^{-1}+\langle T\rangle). \quad (4.16)$$

As for improving the treatment of small rings, it is an easy matter to modify the numerical procedures to use the more accurate equation of motion

$$M_{\rm ion}\dot{v}+\dot{p}_{\rm ring}=eE-\alpha[1-R_{\rm ion}/(\pi R)]\ln(R/\xi)-\zeta f_{\rm ion}(v) \quad (4.17)$$

for the time just subsequent to a nucleation event. The momentum $p_{\rm ring}$ is the impulse of the ring with a trapped ion.[10] During this time also the escape rate P_e varies somewhat; this effect can be incorporated by replacing the probability $P_e\exp[-P_e(t)]dt$ by

$$P_e(t)\exp[-\int_0^t P_e(t')dt']dt\,,$$

as in (4.14) and (4.15).

F. Comparison with Experiment

There is, unfortunately, a paucity of published data on drift velocities for $E\gtrsim E_{c2}$. The theory does, however, provide quite satisfactory agreement with available data. In Fig. 6 the results of calculations incorporating all the extensions discussed above are compared with experimental data[24] at two temperatures.

Consider the results for $T=1.18\,^\circ$K. Curve (a) was obtained using the extrapolation of Cade's data discussed in Sec. IV B. The other parameters were fixed as follows: α using the formula of HO, corrected for the temperature dependence of Δ; $R_{\rm ion}$ and ζ from Table I; $M_{\rm ion}$ from Dahm and Sanders[30]; ΔF_0 from DR; $v_{c1}^{\rm nuc}$ by matching the point $E=E_{c1}$, $v_d=v_{c1}$ (resulting values of $v_{c1}^{\rm nuc}$ are close to but a little smaller than those calculated by DR). It is also necessary to make a rough extrapolation of $f_{\rm ion}(v)$ for $v>v_{c1}$; the results are not, however, sensitive to the manner in which this is done. Note that this calculation therefore contains essentially no free parameters.

In a previous paper,[31] we obtained a satisfactory fit for $E\gtrsim E_{c2}$. The present, more accurate, treatment of small rings has enabled us to fit the data for all fields $\gtrsim E_{c1}$. It is now apparent, however, that the predicted values of the drift velocity are consistently a little low. The most probable source of this error is our extrapolation of Cade's escape data from 0.5 to 1.2 °K. One might, for example, think that the preexponential "attempt rate" Ω_e in Eq. (4.5) for P_e should be temperature dependent. Plotted as curve (b) in Fig. 6 is the predicted drift velocity if Ω_e is increased by a factor of 1.6. Agreement with experiment is now almost perfect. As pointed out previously,[31] the author feels that this sort of comparison would be a good first use of the theory described here. Given the drift velocity for a given E and T, one can in fact uniquely calculate the escape rate, provided only that P_e can be assumed constant in time (Sec. IV B). Since P_e relates directly to details of the ion-vortex interaction, it is of fundamental importance, and the above method will allow its determination in unexplored regions of field and temperature.

The data for $T=1.30\,^\circ$K are in a way more interesting because v_d is now so large that the small-ring effects can no longer be considered corrections—the rings are almost always small! Considering the phenomenological nature of our treatment of small rings, the relatively close agreement with theory is gratifying. The parameters for the theoretical curve were determined in the same way as for the

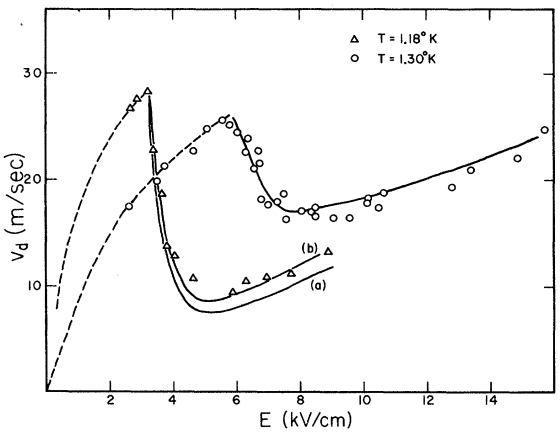

FIG. 6. Comparison of the theory with the experiments of Ref. 24. Curve (a) through the 1.18 °K data is a zero-parameter fit. For curve (b) and the curve through the $T=1.30$ °K data, the escape rates obtained from Ref. 26 have been scaled by a constant factor of 1.6. The drag force on a bare ion was obtained from the data (dashed curves).

lower-temperature data, and the larger value of Ω_e was used.

The portion of the drift-velocity curve for E near E_{c1} is especially sensitive to our assumptions about the physics of the bare ion and small rings. In particular, the results test the form (3.1) for the nucleation rate derived from the theory of DR.

The author would like to point out that the data[24] of Bruschi *et al.*, while providing an interesting illustration of most of the physics discussed in this paper, are not ideally suited for determining escape rates because of the importance of the small-ring effects which are only imperfectly known. Ideally, one would like to begin with drift-velocity data from regions where the drift velocities are somewhat smaller and ring sizes larger. Then, having gathered information regarding the escape rates, one could use the theory, or similar theories, to investigate regions where v_d is large and thus obtain an accurate insight into the behavior of small rings.

G. Persistence Current

One can also calculate other quantities of interest such as the persistence current, reported[2] by Bruschi, Maraviglia, and Mazzoldi (BMM), which is a consequence of the possibility of very large rings arriving at d and then propagating a macroscopic distance χ through a field-free region. Every ion arrives at d, and once the ion is in the field-free region there is little danger it will escape from its ring. The crucial consideration is whether the ion is bound in a ring large enough to propagate the extra distance χ under its own power. With eE set equal to zero, Eq. (4.1) is easily integrated to give the range

$$\chi = \tfrac{1}{2}K^2\rho_s\alpha^{-1}R_0 \tag{4.18}$$

for a ring with a large initial radius R_0. The persistence current consists of all rings which arrive at d in a ring with $R \geq R_0$. Therefore, the quantity to be substituted for Q_h in Eq. (4.7) is

$$i^{(N)}(t_1, t_2, \cdots, t_N) = \begin{cases} i(0), & \text{if } R(d - x(t_1) - x(t_2) - \cdots - x(t_N)) \geq R_0 \\ 0, & \text{otherwise,} \end{cases} \tag{4.19}$$

where $i(0)$ is the total current ad d and $R(x)$ is the inverse to the function $x(R)$ defined in (4.2). The persistence current is therefore given by

$$i(\chi) = i(0)\left[P^{(0)} + \sum_{N=1}^{\infty} \int_0^{t(d-x(R_0))} dt_1 \int_0^{t(d-x(t_1)-x(R_0))} dt_2 \cdots \int_0^{t(d-x(t_1)-\cdots-x(t_{N-1})-x(R_0))} dt_N P^{(N)}(t_1, t_2, \cdots, t_N) \right] \times \theta(R(d) - R_0), \tag{4.20}$$

where R_0 is related to χ by (4.18). If the times are relabeled as $\tau_i = t_{N-i+2}$ for $i = 2, 3, \cdots, N$ and $\tau_1 = t(d - x(t_1) - \cdots - x(t_N))$ then (4.20) assumes the simpler form

$$i(\chi) = i(0)\left[P^{(0)} + \sum_{N=1}^{\infty} \int_{t(R_0)}^{t(d)} d\tau_1 \int_0^{t(d-x(\tau_1))} d\tau_2 \cdots \int_0^{t(d-x(\tau_1)-\cdots-x(\tau_{N-1}))} d\tau_N P^{(N)}(\tau_1, \tau_2, \cdots \tau_N) \right] \times \theta(R(d) - R_0), \tag{4.20'}$$

and (4.20′) can be further reduced as in (4.11).

Equation (4.20), like Eq. (4.10) for the mean drift time, is not useful if P_e is large. We can, however, argue in a similar fashion as previously. Call parts of an ion history between consecutive escapes "epochs." The state of the ion at d will be uncorrelated with its state at distant parts of the history — that is, parts separated from d by, on the average, many epochs. If the average total number of epochs or escapes is large, then characteristics of the beam emerging at d will be independent of d and will depend only on the statistical distribution of the different types of epochs. What we are interested in in this case are the epochs during which the ring exceeds the size R_0. To get the persistence current, the probability of each such epoch must be reduced by the actual fraction of the epoch where $R \geq R_0$. Thus $i(\chi)$ is given by

$$i(\chi) = i(0) \int_{t(R_0)}^{\infty} dt\, P_e \exp(-P_e t) \times [x(t) - x(R_0)]/\langle x \rangle. \tag{4.21}$$

The appropriate fraction of the epoch is the fraction of the *distance* because we are investigating the beam at a fixed distance d.

If $P_n \sim P_e$, then the bare-ion stage must be counted in each epoch. The average extent of the epoch is increased to $\langle x \rangle + \langle X \rangle$ and this term then replaces the denominator in (4.21).

Equation (4.21) is useful only at relatively low temperatures ($\lesssim 1$ °K) because, if there are many

escapes, a given ring is unlikely to survive long enough to gain sufficient energy to propagate a macroscopic distance. (At low temperatures it is possible to apply fields much larger than the drag forces and so create a "persistent" ring in a short distance.)

H. Persistence Current Characteristics

It is inconvenient experimentally to vary the range χ with E and T held fixed. Rather one would like to measure a current-field characteristic for fixed temperature and range. Some results of calculations with (4.20) and (4.21) are shown in Fig. 7. Pictured are persistence characteristics for positive ions for T near 0.85 °K. The escape rates are taken from the fit to Cade's data (Sec. IV B) and d is 1 cm. A persistence current first appears when $R(d) \geq R_0$ and comprises ions which have suffered no escapes. If the escape probability is substantial, as in this case, such ions are very few, however. The persistence current appears gradually as the field is increased to the point where a substantial number of ions suffering multiple escapes are nevertheless able to achieve a size $\geq R_0$ during the final ring stage. Bigger rings go slower, however, and the ion tends to spend more time in the higher field. This effect, combined with the increase in P_e with field, eventually overcomes the effect of the gain in ring size and the persistence current falls toward zero.

Figure 8 is a similar plot for negative ions with $T \sim 1.2$ °K. The escape rates were obtained from the crude estimate of Sec. IV B. The quantity $P_e t(d)$ is relatively small and the threshold behavior is pronounced. Because the fields are larger, P_e now increases more rapidly with the same fractional increase in field and there is at best only a slight increase in current before the effect of escapes wipes out the persistence current.

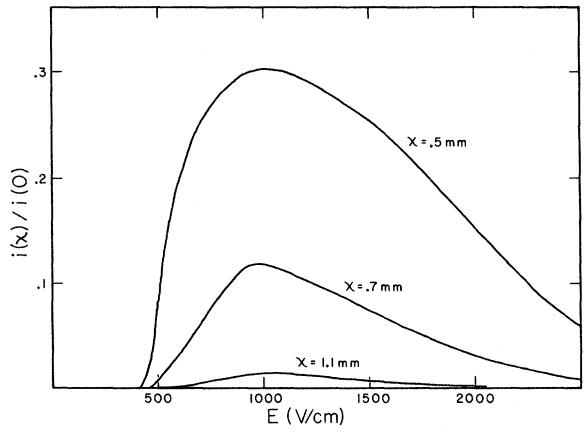

FIG. 7. Persistence currents for the positive ion for three ranges χ, and T near 0.85 °K.

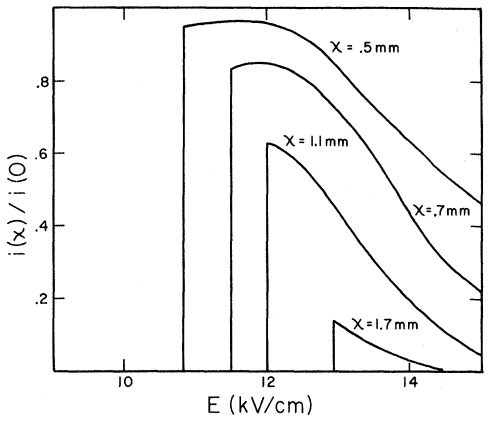

FIG. 8. Persistence currents for the negative ion for several ranges, and T near 1.2 °K.

The larger-range persistence currents decrease with field from the outset.

Let us note here two more novel features of the persistence current. Suppose the same potential is applied over two distances $d_1 < d_2$ and let the corresponding persistence currents (for a given range) be i_1 and i_2. The dissipative losses are smaller for the smaller distance and, because the available energy is the same, larger rings are produced. Therefore, provided P_e is not strongly field dependent, the persistence currents will satisfy the inequality $i_1 > i_2$. (Of course if P_e increases rapidly with field, escapes will cancel the dynamical gains and the inequality will be reversed.) More remarkably, even if the same *field* is applied over the two distances, it can happen that once again the larger current is observed for the smaller distance. This happens, for example, if $R(d_1)$ is not much larger then R_0, if $P_e t(d_1) \sim 1$, and if $P_e t(d_2) \gg 1$. When $d = d_1$, the fraction of zero-escape histories is $\epsilon = \exp[-P_e t(d_1)]$, and because of the first condition $i_1 \approx \epsilon i(0)$. For $d = d_2$, the fraction ϵ is, because of the third condition, very nearly the fraction of epochs with an extent exceeding d_1. However the location of the beginning of the last epoch is uncorrelated with the location $x = d_2$ and, as we argued before, only a fraction δ of these epochs contribute to the persistence current. Hence $i_2 \approx \epsilon\delta i(0) \approx \delta i_1$. Because of the second condition, $\epsilon \sim \delta \sim e^{-1}$, so the effect can be fairly pronounced.

J. Stopping Fields

If the electric field in the persistence region is not zero but finite, and opposes the motion of the ions, then the persistence current will be reduced. The reduction is effected by two mechanisms: energy loss from work done against the field, and escape of the ion from the ring.

If a ring of radius R' enters a region with a stopping field E_s, then we obtain the following equa-

tions similar to (4.2a) and (4.2b) for the time and distance as a function of R:

$$t_s(R, R') = 2\pi\rho_s\kappa\alpha^{-1}\xi^2 \exp(-2\tilde{E}_s)\,[E_1(2\tilde{F}) - E_1(2\tilde{F}')]\,, \tag{4.22a}$$

$$x_s(R, R') = \tfrac{1}{2}\kappa^2\rho_s\alpha^{-1}\{\xi\tilde{E}_s \exp(-\tilde{E}_s)\,[E_1(\tilde{F}') - E_1(\tilde{F})] - R + R'\}\,. \tag{4.22b}$$

Here $\tilde{F} = -\tilde{E}_s - \ln(R/\xi)$ and $\tilde{F}' = -\tilde{E}_s - \ln(R'/\xi)$.

If a ring is to propagate the distance χ in the presence of the stopping field, it must enter the persistence region with $R \geq R_s$, where R_s is given by

$$x_s(R_{\mathcal{E}}, R_s) = \chi \tag{4.23}$$

and $R_{\mathcal{E}}$ is the radius of the smallest allowed ring (Sec. III C). The radius R_s increases with E_s and the current will be completely stopped if R_s exceeds $R(d)$. If escapes are important in the field E but not in the field E_s, then the persistence current is

$$i_s(\chi) = i(\chi_s)\,, \tag{4.24}$$

where $\chi_s \equiv \frac{1}{2}\kappa^2\rho\alpha^{-1}R_s$ and i is given by (4.20) or (4.21). If escapes are important in both regions, then

$$i_s(\chi) = \int_{R_s}^{\infty} dR'\, n(R') \exp[-P_{e,s}t_s(\chi, R')]\,. \tag{4.25}$$

Here $n(R')\,dR'$ is the fraction of rings arriving at d with radius between R' and $R' + dR'$. The function $t_s(x, R')$, obtained from (4.22), is the time it takes a ring of initial radius R' to propagate a distance x in the stopping field. The parameter $P_{e,s}$ is the escape rate in the stopping field and R_s is related to χ by (4.23). The exponential factor is just the probability there is no escape in the persistence region; if there is even one escape the ion is removed from the persistence current. Since $i(\chi) = \int_{R_0}^{\infty} n(R')\,dR'$, we can write $n(R_0) = -di/dR$ so (4.25) becomes

$$i_s(\chi) = -\int_{R_s}^{\infty} dR'\, di/dR' \exp[-P_{e,s}t_s(\chi, R')]\,. \tag{4.26}$$

This form clearly reduces to (4.24) if $P_{e,s} \to 0$. Differentiation of (4.20′) and (4.21) and substitution in (4.26) leads to these final forms suitable for numerical evaluation:

$$i_s(\chi) = i(0)\left(P^{(0)} \exp[-P_{e,s}t_s(\chi, R(d))] + \sum_{N=1}^{\infty} \int_{t(R_s)}^{t(d)} d\tau_1 \exp[-P_{e,s}t_s(\chi, R(\tau_1))] \times \int_0^{t(d-x(\tau_1))} d\tau_2 \cdots \int_0^{t(d-x(\tau_1)-\cdots-x(\tau_{N-1}))} d\tau_N \times P^{(N)}(\tau_1, \tau_2, \ldots, \tau_N)\right)\theta(R(d) - R_s)\,, \tag{4.27}$$

and if $P_e \to \infty$, $P_{e,s} \to \infty$, then

$$i_s(\chi) = i(0) \int_{x(R_s)}^{\infty} dx \exp[-P_{e,s}t_s(\chi, R(x)) - P_e t(x)]/\langle x\rangle\,. \tag{4.28}$$

[The expected limit of (4.28) for $P_{e,s} \to 0$ can be recovered after a partial integration.]

K. Discussion of Experiments

Besides having intrinsic interest, experiments testing the predicted current characteristics would lend a degree of redundancy to the determination of escape rates discussed in Sec. IV F. Unfortunately, the data of BMM are not quantitative and are contaminated by other effects.[23]

In this regard, experimenters should be warned[23] that unusual care must be taken to ensure that the ion beam is well collimated and that the only losses are due to escapes and drag forces as described above. For example, in a retarding electric field the vortex motion is unstable[32] in that a small initial error in angle between the direction of propagation and the direction of the field tends to grow; the ion beam spreads out and can even be reversed in this fashion. Even in accelerating fields space charge and defocussing effects at the grids can be severe.

Nevertheless, Little[33] has reported preliminary persistence results which agree with the interpretation presented here. In particular, Little's currents exhibit a cutoff which corresponds to the sieving action of his grids on the very large rings we have supposed to be responsible for the current.

While it is difficult to draw any definite conclusions from the data of BMM, it is interesting that their current characteristic for negative ions near 0.9 °K somewhat resemble the initial part of our curves (Fig. 7) for the *positive* ion where the escape probability is ~1 sec^{-1}. It is amusing to note that this suggestion of an anomalously high (the estimate in Sec. IV B gives $P_e < 10^{-5}$ sec^{-1}) negative-ion escape rate has been echoed by Douglass's[34] reporting work on rotating He II.

BMM also conducted an investigation of second sound attenuation, which should be proportional to

the total length of vortex line present. This sort of experiment is much less sensitive to errors associated with a messy beam. Their main result, a linear field dependence of the attenuation (normalized to the source current), is easily explained by reference to the result (Sec. IV A) that for large $\tilde{E}$ the ring radius varies linearly with field.

L. Summary of Definitions

Here a number of the functions introduced in this section are summarized for the reader's convenience:

time for a ring in an electric field E to grow to a radius R starting with a small radius, $t(R)$;

inverse of the above, the radius attained in the time t, $R(t)$;

distance needed to grow to a radius R, $x(R)$;

radius attained in the distance x, $R(x)$;

distance covered in time t, $x(t)$;

time covered in distance, x, $t(x)$;

time for a ring to shrink from radius R' to R in a stopping field, $t_s(R, R')$;

distance covered while a ring shrinks from radius R' to R in a stopping field, $x_s(R, R')$;

time required to go a distance x with initial radius R' in a stopping field, $t_s(x, R')$;

persistence current observed for a range χ with zero stopping field, $i(\chi)$;

persistence current for a range χ in a nonzero stopping field, $i_s(\chi)$.

The integration of all differential equations not explicitly integrated in this paper, the evaluation of all integrals not explicitly evaluated, the solution of various parametric equations, and the inversion of some functions were carried out on an electronic computer using standard methods. A rational approximation[25] to the exponential integral was used.

ACKNOWLEDGMENT

The author would like to thank Dr. R. E. Little for his part in many discussions and a number of valuable ideas.

---

*Present address: Laboratory of Atomic and Solid State Physics, Cornell University, Ithaca, N. Y.

[1]K. Huang and A. C. Olinto, Phys. Rev. 139, A1441 (1965).

[2]L. Bruschi, B. Maraviglia, and P. Mazzoldi, Phys. Rev. 143, 84 (1966).

[3]For example, F. Reif and L. Meyer, Phys. Rev. 119, 1164 (1960); G. Careri, S. Cunsolo, and P. Mazzoldi, *ibid.* 136, A303 (1964); and more recently, K. Schwarz, Phys. Rev. Letters 24, 641 (1970); M. Steingart and W. I. Glaberson, Phys. Rev. A 2, 1480 (1970); L. Bruschi and M. Santini, Rev. Sci. Instr. 41, 102 (1970).

[4]D. M. Strayer, R. J. Donnelly, and P. H. Roberts, Phys. Rev. Letters 26, 165 (1971); D. M. Strayer and R. J. Donnelly, *ibid.* 26, 1420 (1971).

[5]J. A. Cope and P. W. Gribbon, Phys. Letters 16, 128 (1965); B. K. Jones, Phys. Rev. 186, 168 (1969).

[6]G. Careri, S. Cunsolo, and P. Mazzoldi, Phys. Rev. Letters 7, 151 (1961), and Ref. 3.

[7]J. A. Cope and P. W. Gribbon, in *Proceedings of the Ninth International Conference on Low-Temperature Physics, Columbus, Ohio,* 1964, edited by J. A. Daunt *et al.* (Plenum, New York, 1965).

[8]Schwarz, Ref. 3; Steingart and Glaberson, Ref. 3.

[9]G. Careri, S. Cunsolo, P. Mazzoldi, and M. Santini, in Ref. 7.

[10]R. J. Donnelly and P. H. Roberts, Phys. Rev. Letters 23, 1491 (1969).

[11]Equation (2.8) can have two roots (see Ref. 1). The large root should be rejected because it corresponds to a situation of unstable equilibrium: If the velocity is infinitesimally larger than the large root, then the complex will shrink and break up, and if the velocity is slightly smaller, the ring grows and $v \to v_{eq}^{ir}$ (the small root). See Secs. III C and III D.

[12]G. W. Rayfield and F. Reif, Phys. Rev. 136, A1194 (1964).

[13]The factor ζ very likely does depend on v. In particular one expects $\zeta \to 1$ for $R/R_{ion} \to 0$. Our choice corresponds to an average over the region of interest. HO estimate in a footnote that $\zeta \approx \frac{1}{3}$ but appear to have used $\zeta \approx 0.22$ in their Eq. (24) and subsequent calculations.

[14]C. Careri *et al.*, cited in HO; L. Bruschi, P. Mazzoldi, and M. Santini, Phys. Rev. Letters 21, 1738 (1968).

[15]J. L. Yarnell, G. P. Arnold, P. J. Bendt, and E. C. Kerr, Phys. Rev. 113, 1379 (1959).

[16]K. Schwarz and R. Stark, Phys. Rev. Letters 21, 967 (1968); 22, 1278 (1969); G. Baym, R. G. Barrera, and C. J. Pethick, *ibid.* 22, 20 (1969).

[17]R. J. Donnelly and P. H. Roberts, Proc. Roy. Soc. (London) A312, 519 (1969).

[18]S. Cunsolo and B. Maraviglia, Phys. Rev. 187, 292 (1969).

[19]The energy of the ring was calculated according to the formulae of DR. One can also use the following approximation, useful for $R \gtrsim \frac{1}{2}R_{ion}$, and derived by the same reasoning that led to Eq. (2.11) for f_{ir}: $\mathcal{E}_{ir} = [1 - R/(\pi R_{ion})]\mathcal{E}_{ring} + \frac{1}{2}M_{ion}v^2$. Here $\mathcal{E}_{ring} = \frac{1}{2}\kappa^2\rho_s R[\ln(R/\xi) - \frac{3}{2}]$ is the energy of a bare vortex ring. The mass M_{ion} is taken as the effective mass, including the hydrodynamic mass. We have neglected the possibility that, because the hydrodynamic energy density is quadratic in the local fluid velocity, the hydrodynamic mass may be modified by the presence of the ring. This is a correct procedure for very small and very large rings and hopefully not too bad in between.

[20]D. A. Neeper and L. Meyer, Phys. Rev. 182, 223 (1969); M. Kuchnir, J. B. Ketterson, and P. R. Roach, Phys. Rev. Letters 26, 879 (1971).

[21]This explanation requires $v_{c1}^{nuc} \sim 20$ m/sec for the positive ion, considerably smaller than the prediction of DR, but consistent with the observed value for negative ions, for which the v_d curve is "normal" (filled circles in Fig. 4).

[22]M. Kuchnir (private communication).

[23]R. E. Little (private communication).

[24]Bruschi *et al.*, Ref. 14.

[25]*Handbook of Mathematical Functions,* edited by M. Abramowitz and I. A. Stegun (U. S. GPO, Washington,

D.C., 1966), Chap. 5.
[26]A. G. Cade, Phys. Rev. Letters 15, 238 (1965).
[27]R. L. Douglass, Phys. Rev. Letters 13, 791 (1964).
[28]In most cases where this correction is important, P_n^{-1}, while small, is large compared to the time required to accelerate the bare ion to a velocity near v_{eq}^{ion}, so that $P_n(v)\exp[-\int_0^T P_n(v')\,dT']$ can be replaced by $P_n(v_{eq}^{ion})\times\exp[-P_n(v_{eq}^{ion})T]$ and we have $\langle T\rangle\approx[P_n(v_{eq}^{ion})]^{-1}$, $\langle X\rangle\approx v_{eq}^{ion}\langle T\rangle$.
[29]The only exception is a single narrow region of field and temperature near $E=E_{c1}$ and T such that $P_e(E_{c1}, T)\sim\tau_d^{-1}$. This case can be treated by a straightforward generalization of Eq. (4.10).
[30]A. J. Dahm and T. M. Sanders, Jr., Phys. Rev. Letters 17, 126 (1966).
[31]T. C. Padmore, Phys. Rev. Letters 26, 63 (1971).
[32]K. W. Schwarz, Phys. Rev. 165, 323 (1968).
[33]R. E. Little, Bull. Am. Phys. Soc. 16, 639 (1971).
[34]R. L. Douglass, Phys. Rev. 165, 323 (1968).

PHYSICAL REVIEW A VOLUME 5, NUMBER 1 JANUARY 1972

Ultraviolet Emission Spectrum of Electron-Bombarded Superfluid Helium*

M. Stockton, J. W. Keto, and W. A. Fitzsimmons
University of Wisconsin, Madison, Wisconsin 53706
(Received 23 June 1971)

The emission spectrum of electron-bombarded superfluid helium has been measured as a function of wavelength between 600 and 1100 Å. The spectrum is characterized by a very intense band of continuous emission peaking at approximately 800 Å, along with a series of less intense bands between the wavelengths of 600 and 710 Å. This continuum is interpreted in terms of the radiative dissociation of neutral helium molecules in the reaction $A\,^1\Sigma_u^+\rightarrow X\,^1\Sigma_g^+$. The over-all intensity corresponds to about 5×10^{15} (photons/sec)/μA of 160-keV electron beam excitation. The uv fluorescence of electron-bombarded superfluid helium is by far the most intense emission of the excited liquid and may represent a useful source of uv light.

I. INTRODUCTION

Considerable experimental effort has been directed toward the fast-particle bombardment of liquid helium as a method of studying the microscopic structure of simple liquids. The possible existence of identifiable neutral electronically excited states of the liquid is of particular interest since it is expected that such excitations could be used to probe the liquid structure. The experimental results presented in this paper indicate that the $A\,^1\Sigma_u^+$ state of the neutral helium molecule is the neutral excitation that is most readily produced in electron-bombarded superfluid helium.

The scintillation of liquid helium in the vacuum ultraviolet due to α-particle excitation was studied by Moss and Hereford almost a decade ago.[1] On the basis of an apparent inhibition of this scintillation below the λ temperature, these authors suggested the possible existence of excited atomic and perhaps even metastable states of the liquid. At about the same time, Jortner *et al.* provided additional evidence of neutral excitations in liquid helium by observing the enhanced emission of oxygen and nitrogen impurities in the liquid when subjected to α-particle bombardment.[2] These authors proposed the existence of an efficient energy-transfer mechanism to the colloidally suspended impurities. These suggestions have been supported by the observations of Surko and Reif which established the existence of long lived but as yet unidentified neutral excitations in superfluid helium.[3] The question of identifying the nature of the electronic excitations in liquid helium has been very difficult due to a lack of sufficient intensity to allow spectroscopic measurements.

More recently, electron beams have been used to excite liquid helium. This experimental method has the advantage that the levels of particle bombardment can be substantially greater than what is attainable with a manageable radioactive source. In addition the transient behavior of the excitations produced in the liquid can be studied by pulsing the source of electrons. The use of electron beams has made possible the first direct spectroscopic identification of electronically excited atomic and molecular states in liquid helium.[4-6] The localized nature of the excitations is demonstrated by the vibrational and rotational structure of the observed helium molecular fluorescence.[7] These experiments have shown that large concentrations of both the atomic $2\,^3S$ and molecular $a\,^3\Sigma_u^+$ metastable states of helium are present in the excited liquid and they have shown in addition that the lowest bound $A\,^1\Sigma_u^+$ state of He_2 is populated at a rapid rate.[4,6,8] The dynamical properties of the atomic and molecular metastable states in liquid helium have been studied recently through the time dependence of the absorption and emission spectra; however, the present authors discuss this subject in a